Journal of Theoretical and Applied Information Technology
10th August 2014. Vol. 66 No.1

ISSN: 1992-8645 www.jatit.org E-ISSN: 1817-3195

PID CONTROLLER FOR NARX AND ANFIS MODELS OF MARINE PIPE CYLINDER UNDERGOES VORTEX INDUCED VIBRATION

[1]MOHAMMED JAWAD MOHAMMED, [2]INTAN Z. MAT DARUS
[1]Faculty of Mechanical Engineering, UTM, Skudai, Johor, Malaysia-81310
[1]Faculty of Electromechanical Engineering, University of Technology, Baghdad, Iraq
[2] Faculty of Mechanical Engineering, UTM, Skudai, Johor, Malaysia-81310
E-mail: [1]msc.mohammed83@gmail.com, [2]intan@fkm.utm.my

ABSTRACT

PID controller discrete time on marine cylinder pipe risers which represented based on system identification models under vortex induced vibration (VIV) has been verified in this work. Input-output data have been provided from the experimental setup of previous paper. Two System identification methods used to create models which are: Neural Network based on Nonlinear Auto-Regressive External (Exogenous) Input (NARX) and Adaptive Neuro-Fuzzy Inference System (ANFIS). NARX and ANFIS models have selected based on Mean Square Error (MSE) technique. While, PID controller has been applied to overcome on the pipe cylinder oscillation for all models. Also, the controller performance has been compared on each model during from tuning the controller parameter (K_P, K_I and K_D) depending on the heuristic method and validation the gain values based on Mean Square Error (MSE) technique. Finally, the consequences demonstrated that the ANFIS model better than the NARX model to forecast the dynamic behavior of the system. By contrast, PID controller has been managed to decrease the pipe cylinder fluctuation for all models specially the NARX model system identification.

Keywords: *System Identification, NARX Model, ANFIS Model, PID Controller, Vortex Induced Vibration*

1. INTRODUCTION

Vortex Induced Vibration (VIV) is one of the problems which lead to the fatigue damage in the offshore applications field such as pipeline and risers because of the dynamic behavior which is mounted on the pipe cylinder [1][2]. VIV is a result of the interaction between the bluff body and the vortices shedding behind the structure. Whereas, the vortices generate a force cause to oscillate the cylinder transversely and perpendicular direction for the water flow. This phenomenon will be very risky when the vortex shedding frequency closes to the natural frequency for the cylinder under water (resonance circumstance) [3].

Depending on the semi-empirical model methods, the VIV behavior in marine engineering application can be explained into three main headings [4]. Firstly, the model which studies the relationship between fluid oscillator and the cylinder oscillator equations to predict the dynamic response of the model is called wake oscillator model [5]. Secondly, the model which uses the single dynamic equation with aero-elastic term to predict the model is called a single degree of freedom model. Finally, previous research study the measuring of the force components on the body is called force-decomposition model [6]. However, there are two ways in this field can suppress the oscillation of a pipe cylinder under VIV which is: passive and active vibration control during from adding stiffness or mass without the external power or using sensors and actuators as an external power to the system respectively [7]. The active method is very wide use up to now because of its cheaper and produce a higher performance comparison with the passive method. The first endeavor was by Baz and Ro (1991) [8].

For the time being, few researches in this field used the controlling methods to decrease the attenuation of VIV on pipe after representing the system characteristic during from system identification models [9]. System identification methods used to predict the system model in a time or frequency model as a transfer function or equivalent mathematical model whether the system behavior was linearized or non-linearized [10].

In this work, the attenuation process of VIV on marine risers has been branched into four main segments: firstly, obtained the input-output data of the experimental work from the preceding paper. Secondly, apply NARX and ANFIS as a system

Journal of Theoretical and Applied Information Technology
10th August 2014. Vol. 66 No.1

ISSN: 1992-8645 www.jatit.org E-ISSN: 1817-3195

identification method to forecast the dynamic model behavior for the system before validating the outcomes during from MSE technique. Thirdly, study the effectiveness of PID controller discrete time on NARX and ANFIS models. Finally, discuss the work outcomes.

2. EXPERIMENTAL DATA

In this study, the input-output data extracted from previous paper by Shaharuddin and Mat Darus [11] [12]. The researchers used the rigid cylinder with flexibly supporting in the crossflow vibration only. Table 1 showing the description and the parameter values which calculated from experimental test.

Table 1. Obtained parameters [11][12]

Parameter	Symbol	Value	Unit
Cylinder Diameter	D	50	mm
Cylinder Length	L	1110	mm
Aspect Ratio	L/D	22.2	Dimensionless
Cylinder mass	m	2.95	kg
Mass ratio	m*	1.18	Dimensionless
Natural Frequency	fw	1.11	Hz
Damping ratio in water	ζ	0.1007	Dimensionless
Stiffness	k	265.34	N/m

Input (from accelerometer A) and output (from accelerometer B) data obtained from Shaharuddin and Mat Darus as shown in Figure 1 which included 33000 data for input and output data[11][12].

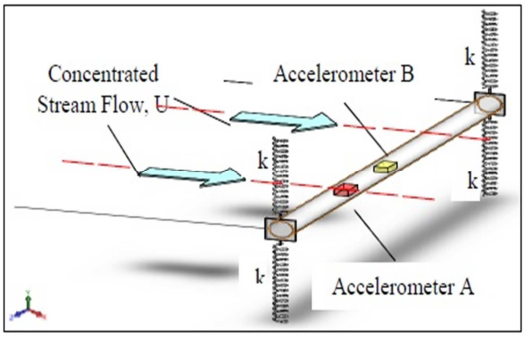

Figure 1. Accelerometer Positions For Detecting And Observing Data Of Experimental Setup Diagram [11][12]

Accelerometer A represents the detected input data for system identification. While, accelerometer B is represents the observed output for system identification. In Figure 2 and 3 shown the relationship between the input and output amplitudes with the time

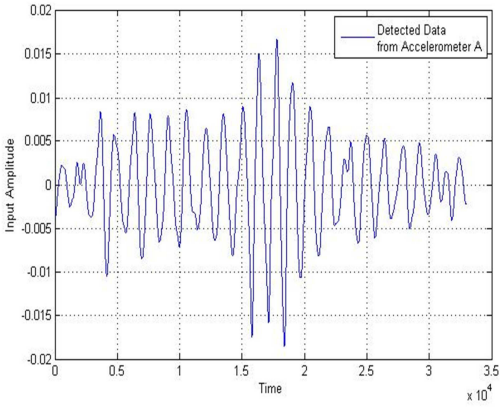

Figure 2. Detected Amplitude With Simple Time Series For Pipe Cylinder

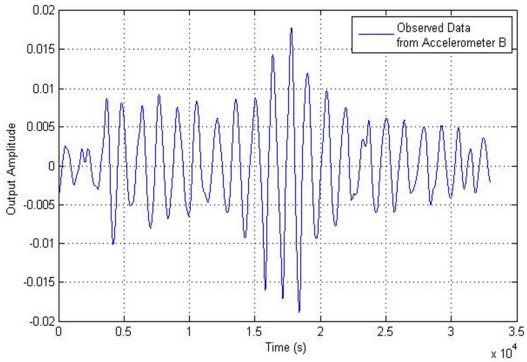

Figure 3. Observed Amplitude With Simple Time Series For Pipe Cylinder

3. SYSTEM IDENTIFICATION

System identification methods: Neural Network based on Nonlinear Auto-Regressive External (Exogenous) Input (NARX) and Adaptive Nero-Fuzzy Inference System (ANFIS) employed to forecast the dynamic response characteristics caused by vortex induced vibration on the marine riser.

2.1 Nonlinear Auto-Regressive External Input Model (NRAX)

NARX model is used for various directions for example control and system identification. Also, it is able to predict the output real time data. The NARX algorithm can be express as follows [13]:

$$y(t) = \frac{B(z^{-1})}{A(z^{-1})}\, u(t) + \frac{\xi(z^{-1})}{A(z^{-1})} \qquad (2)$$

where

ISSN: 1992-8645 www.jatit.org E-ISSN: 1817-3195

$$A(z^{-1}) = 1 + a_1 z^{-1} + \cdots + a_n z^{-n} \quad (3)$$

$$B(z^{-1}) = b_0 + b_1 z^{-1} + \cdots + b_n z^{-(n-1)} \quad (4)$$

After neglecting the noise error and defining the $B(z^{-1})$ and $A(z^{-1})$:

$$y(t) = f[y(t-1), \ldots, y(t-n_a), .., u(t-n_k), .., u(t-n_k-n_b+1)] \quad (5)$$

n_a, n_b are represent the previous value of input and output respectively. While, the n_k represents the input delay. Finally, f represents the nonlinear function which can be carried out by using intelligent methods such as neural network.

2.2 Neural Network Time Series

Neural Network is one of artificial methods which can be used for the nonlinear dynamic system identification. It is consists of a number of neurons arranged in numerous layers. According to Figure 4, Neural Network models include at least three layers which are input, hidden and output layers. The equations can be calculated as follows:

2.2.1 Hidden layer

For hidden layer:

$$v_1 = x_1 w_{11} + x_2 w_{12} + y_1 w_{13} + y_2 w_{14} + b_1 \quad (6)$$

$$v_2 = x_1 w_{21} + x_2 w_{22} + y_1 w_{23} + y_2 w_{24} + b_2 \quad (7)$$

Then

$$f_1 = \frac{1}{1+e^{-v_1}} \quad (8)$$

$$f_2 = \frac{1}{1+e^{-v_2}} \quad (9)$$

where
x_1, x_2 are the actual input data of the input network.
y_1, y_2 are the actual output of the input network.
$w_{11}, w_{12}, w_{13}, w_{14}, w_{21}, w_{22}, w_{23}, w_{24}$ the weights between input and hidden layers.
b_1, b_2 the bias weights for hidden layer
v_1, v_2 the summation values for hidden layer
f_1, f_2 the final values for hidden layer.

2.2.2 Output layer

For output layer:

$$v_3 = f_1 w_{31} + f_2 w_{32} + b_3 \quad (10)$$

$$f_3 = \frac{1}{1+e^{-v_3}} \quad (11)$$

where
w_{31}, w_{32} is the weights between the hidden and output layers.
b_3 is the bias weights for the output layer.
v_3 is the summation values for the output layer.
f_3 is the final predicted value for the output layer or neural network process.

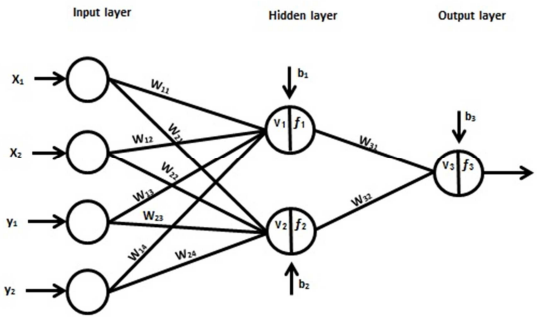

Figure 4 Neural Network Architecture

2.3 Adaptive Neuro-Fuzzy Inference System

In this paper, ANFIS model is utilized to predict the dynamic response of the vibrating pipe cylinder caused by VIV. ANFIS is an adaptive neural network that utilized a fuzzy inference system as an integrated procedure to produce the predicted output. The incoming signals are used as a function and implemented during from the neuron. The Fuzzy Inference System (FIS) includes five main blocks as shown in Figure 5. While Figure 6 shown the architecture of ANFIS model [14].

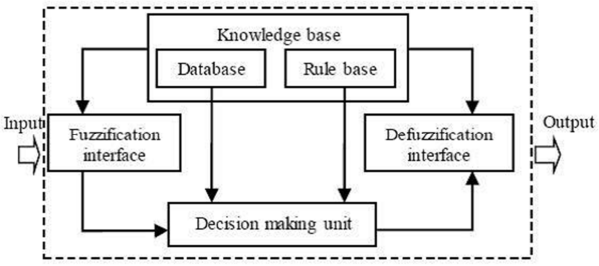

Figure 5 FIS Architecture

Journal of Theoretical and Applied Information Technology
10th August 2014. Vol. 66 No.1

ISSN: 1992-8645 www.jatit.org E-ISSN: 1817-3195

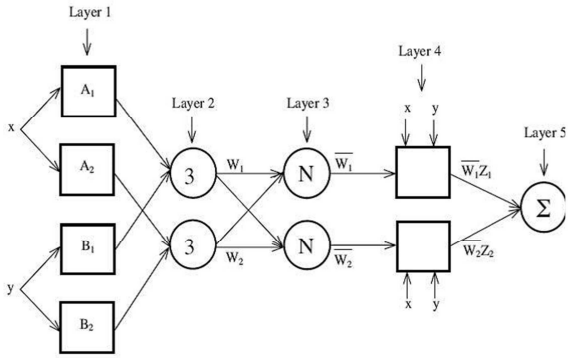

Figure 6 ANFIS Architecture [14]

According to the ANFIS structure, $O_{l,i}$ is assumed as the output for each layer. Whereas i_{th} the output of the node in l_{th} layer. The ANFIS work for each layer as follows:

2.3.1 Layer 1:

In this layer, every node is an adaptive node with parametric function. The membership grade which represents the brittle value is considered the node output. The equation form of this layer is:

$$\mu_{Ai}(x) = \frac{1}{1 + \left|\frac{x + c_i}{a_i}\right|^{2bi}} \quad (12)$$

where a_i, b_i, c_i represent the parameters set and which is referred premise parameters, A represents the linguistic label and x represents the input.

2.3.2 Layer 2:

In this layer, each node is fixed. The output represents the rule's firing strength and the product of the input.

$$O_{L,i} = \omega = \mu(A_i(x).\mu(B_i(x)) \quad (13)$$

2.3.3 Layer 3:

Each node in this layer is a fixed and computes the ratio of rule's firing strength

$$O_{l,i} = \bar{w}_i = \frac{w_i}{w_1 + w_2} \quad (14)$$

2.3.4 Layer 4:

In this layer, the nodes are adaptive and the parameter here called consequent parameters:

$$O_{l,i} = \bar{w}_i f_i = \bar{w}_i(p_i x + q_i y + r_i) \quad (15)$$

2.3.5 Layer 5:

The node in this layer is a single include all signals and the overall output is:

$$O_{l,5} = \sum_i \bar{w}_i f_i = \frac{\sum_i w_i f_i}{\sum_i w_i} \quad (16)$$

2.4 Checking The Results

The verification process of the consequences is considered one of the important ways to measure the performance of the mathematical algorithms which used in this paper. Also, check the algorithm effectiveness to make sure that which one is best from the other. In this paper, Mean Square Error method (MSE) used to verify the results obtained in this work. The equation of Mean Square Error is [15]:

$$\varepsilon(t) = \frac{1}{N}\sum_{t=1}^{N} y(t) - \hat{y}(t)^2 \quad (17)$$

where

$y(t)$ is represents the actual output from the experimental setup.

$\hat{y}(t)$ is represents the predicted output which obtained from system identification methods.

The data which used in this paper are divided into two partitions. The first partition is used for testing and the other partition for validating.

4. PID CONTROLLER

PID controller harnessed to bring down the motion of the pipe cylinder for marine risers under vortex emerged vibration to compute the amount of the error between the output measured and the desired set point under disruptive load as shown in Figure 7. Heuristic method is used to tune the PID parameters (K_I, K_P and K_D). Also, this method has been evaluated based on mean square error (MSE) technique which it's included three steps [16]: firstly, accounting the last proportional gain value (K_P) by considering to variant values until getting this gain to the minimal MSE of the system when being the integral and derivative gain values equal

Journal of Theoretical and Applied Information Technology
10th August 2014. Vol. 66 No.1

ISSN: 1992-8645 www.jatit.org E-ISSN: 1817-3195

to zero. Secondly, calculating for the last integral gain value (K_I) by considering to variant values until getting this gain to the minimal MSE of the system when being the proportional gain equal to the last value for the first step and the derivative value equal to zero. Finally, accounting the last derivative gain value (K_D) by considering to the variant values for this gain until getting it to the minimal MSE of the system when being the proportional and the derivative gain values equal to the last value of the first and second steps respectively. Figure 8 shown the block diagram for marine risers system which it's undergoes in the vortex induced vibration as a distributed load with PID controller discrete time.

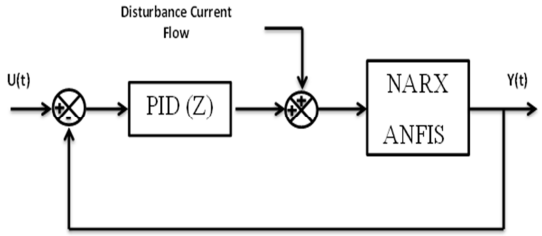

Figure 7 Block Scheme For Controller And System Identification

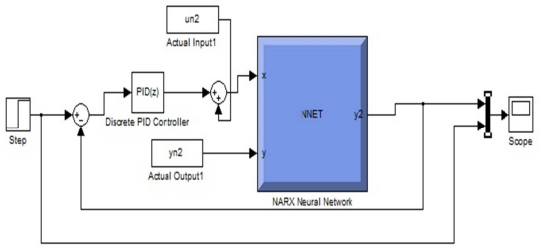

(a)

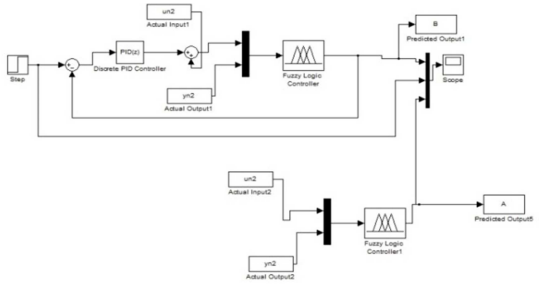

(b)

Figure 8 Block Scheme For Controller With (A) System Identification (NARX) And (B) System Identification (ANFIS)

5. RESULTS AND DISCUSSIONS

5.1 System Identification For NARX Model

Neural Network based on Nonlinear Auto-Regressive external input model (NRAX) has been employed to predict the dynamic response of the system. In this method, 33000 data used as an input and output data which extracted from the experimental setup for prior paper and it's distributed into two inputs and one output. Whereas, all data separated into three portions: firstly, 32100 data. Secondly, 4950 used to validate the system and last part utilized 4950 data for testing. Also, in this paper used different values for the number of neurons (NE) which ranged between 1 to 11 neurons for the default number of delays 2 to find the lower MSE. Then, the best result from pervious process fixed and used for different number of delays until finding the lower MSE which ranged between 1 to 11 values. Based on Table 2, the lowest MSE founded at neurons (NE) 8 is 1.2714×10^{-9} when the numbers of delay have been fixed in 2. While, Table 3 shown that the lowest MSE founded the number of delays 2 is 1.2714×10^{-9} when the number of neurons has been fixed at 8. That's means that the best representation for the NARX model to describe the dynamic response when being the number of neurons and the numbers of delay equal 8 and 2 respectively. Figure 9 and 10 showed the best representation for NARX model at NE equal 8 and number of delay 2 for amplitude and error.

Table 2 Mean Square Error for NARX Model at Number of Delay 2

NE	MSE for training	MSE validated	MSE tested	MSE Overall
1	7.06994×10^{-7}	7.03911×10^{-7}	7.3038×10^{-7}	7.1048×10^{-7}
2	1.51825×10^{-7}	1.46421×10^{-7}	1.6348×10^{-7}	1.5353×10^{-7}
3	2.51148×10^{-9}	2.53456×10^{-9}	2.4949×10^{-9}	3.2278×10^{-9}
4	2.25323×10^{-8}	2.10880×10^{-8}	2.2457×10^{-8}	2.2795×10^{-8}
5	1.90786×10^{-9}	1.88947×10^{-9}	1.9190×10^{-9}	2.2781×10^{-9}
6	2.33170×10^{-8}	2.42179×10^{-8}	2.3911×10^{-8}	2.4056×10^{-8}
7	8.42986×10^{-8}	8.52992×10^{-8}	8.5811×10^{-8}	8.5672×10^{-8}
8	4.7337×10^{-10}	4.7219×10^{-10}	4.7699×10^{-10}	1.2714×10^{-9}
9	3.27642×10^{-9}	3.31040×10^{-9}	3.4166×10^{-9}	4.0278×10^{-9}
10	6.28938×10^{-9}	6.58235×10^{-9}	6.6588×10^{-9}	6.7772×10^{-9}
11	1.60514×10^{-8}	1.62700×10^{-8}	1.7577×10^{-8}	1.6682×10^{-8}

Journal of Theoretical and Applied Information Technology
10th August 2014. Vol. 66 No.1

ISSN: 1992-8645 www.jatit.org E-ISSN: 1817-3195

Table 3 Mean Square Error for NARX Model at Number of Hidden Neuron 8

No. of Delay	MSE for training	MSE validated	MSE tested	MSE Overall
1	1.2692×10^{-8}	1.2709×10^{-8}	1.3011×10^{-8}	1.3078×10^{-8}
2	4.7337×10^{-10}	4.7219×10^{-10}	4.7700×10^{-10}	1.2714×10^{-9}
3	2.3379×10^{-10}	2.2933×10^{-10}	2.3540×10^{-10}	1.3273×10^{-9}
4	6.0016×10^{-9}	6.0448×10^{-7}	5.9680×10^{-7}	6.4521×10^{-9}
5	1.8549×10^{-8}	1.8502×10^{-8}	1.8931×10^{-8}	1.9537×10^{-8}
6	3.0966×10^{-8}	3.1253×10^{-8}	1.0954×10^{-8}	3.2182×10^{-8}
7	3.3785×10^{-8}	3.6127×10^{-8}	3.4293×10^{-8}	3.4956×10^{-8}
8	1.3636×10^{-9}	1.3966×10^{-9}	1.3686×10^{-9}	2.8229×10^{-9}
9	2.0855×10^{-9}	2.0098×10^{-9}	1.9893×10^{-9}	3.7473×10^{-9}
10	2.7858×10^{-9}	2.7113×10^{-9}	2.8606×10^{-9}	2.8790×10^{-8}
11	7.7023×10^{-9}	7.7061×10^{-9}	8.0669×10^{-9}	8.9183×10^{-9}

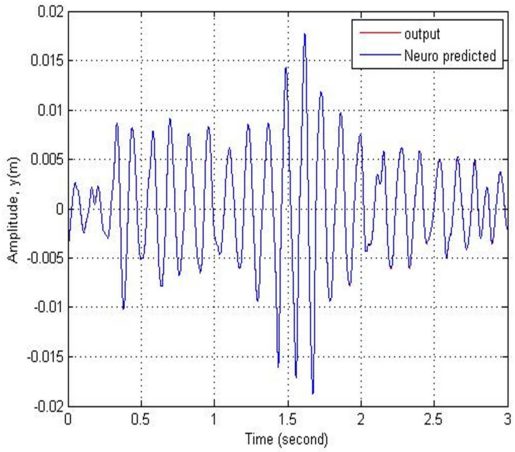

Figure 9 Amplitude of Actual and Predicted Output Depends on NARX

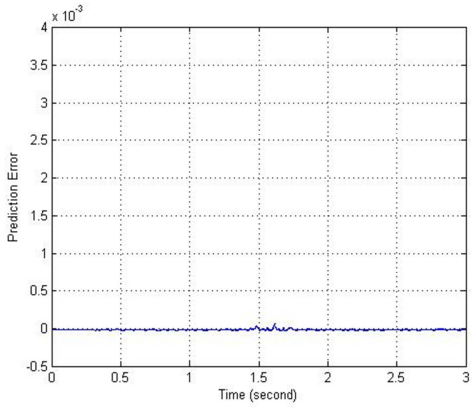

Figure 10 Error of The Predicted Output Depends on NARX

5.2 System Identification For ANFIS model

To compose the ANFIS model in this research, two variable inputs (X and Y) have been used in ANFIS identification. The first step after loading the training data (15000) and checking data (18000) included specifying the number of membership functions (MF) which were two for each input. Then, the generalized bell shape has been selected in this work as a type of MF and this step was a second step to make the FIS model. After generating the FIS model, the third step includes creating the ANFIS model during from selecting the epoch and tolerance values which are represented the iteration number and the error respectively. The final step was evaluating the MF of the model and finding the MSE which amounted to 2.5635×10^{-13}. Table 4 is referring the ANFIS data while Figure 11, 12 and 13 shown the ANFIS architecture, predicted response and the predicted error respectively.

Table 4 ANFIS Data

ANFIS information	Values
Linear parameter number	4
Nonlinear parameter number	12
Total parameter number	24
Training number	15000
Checking number	18000

Journal of Theoretical and Applied Information Technology
10th August 2014. Vol. 66 No.1

ISSN: 1992-8645 www.jatit.org E-ISSN: 1817-3195

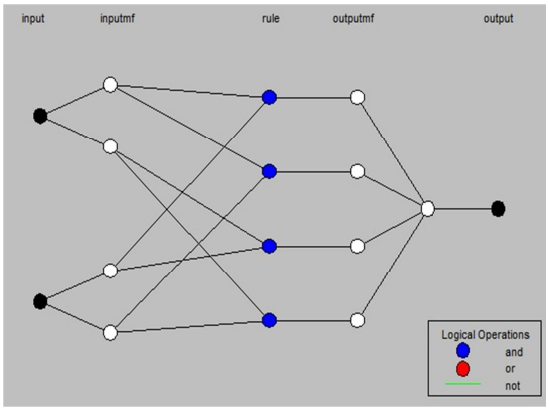

Figure 11 ANFIS Architecture

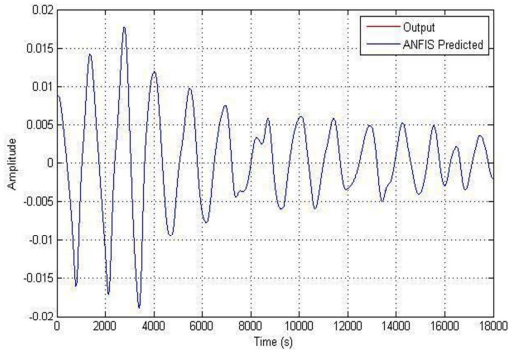

Figure 12 Amplitude of Actual and Predicted Output Depends on ANFIS.

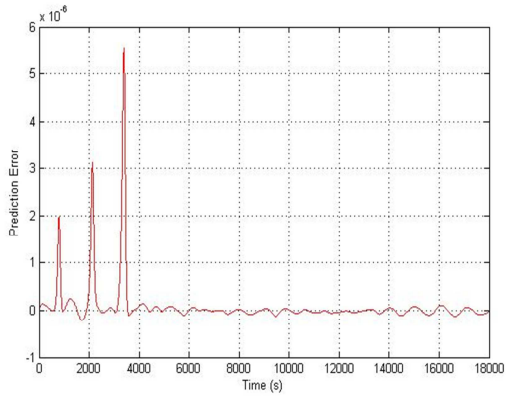

Figure 13 Error of The Predicted Output Depends on ANFIS.

5.3 PID Controller for NARX and ANFIS Models

PID controller has been utilized to reduce the pipe cylinder oscillation caused by VIV which is represented by using NARX and ANFIS system identification models after comparison of the results between system identification models. The PID parameters have been set during of the heuristic method which is consisted finding P gain value at the lowest MSE, then finding PI gain values at lowest MSE and finally finding PID gain values at the lowest MSE. Details of the results divided into two parts: firstly, Table 6 shown the outcomes for NARX which recorded the best magnitude for K_p = -5 at lowest MSE equal $6.147x10^{-6}$. Also, the best magnitude for K_I = -2.5 at lowest MSE equal $3.832x10^{-10}$. While the best magnitude for K_D = -0.2 at lowest MSE equal $3.669x10^{-10}$. According to Figure 14 and 15, the results shown that the PID controller has been succeeded to suppress the effect of VIV comparison with the system performance without controller.

Table 5 PID Parameter Setting For NARX Model By Using MSE

K_P	MSE	K_I	MSE	K_D	MSE
1	8.519×10^{-4}	1	9.15×10^{-4}	1	4.527×10^{-4}
-1	3.353×10^{-4}	-1	1.009×10^{-9}	0	3.832×10^{-10}
-2	4.027×10^{-5}	-1.5	5.633×10^{-10}	-0.1	3.714×10^{-10}
-4	6.718×10^{-6}	-2	4.211×10^{-10}	-0.15	3.682×10^{-10}
-5	6.147×10^{-6}	-2.5	3.832×10^{-10}	-0.2	3.669×10^{-10}
-6	5.687×10^{-4}	-3	4.353×10^{-10}	-0.25	3.677×10^{-10}

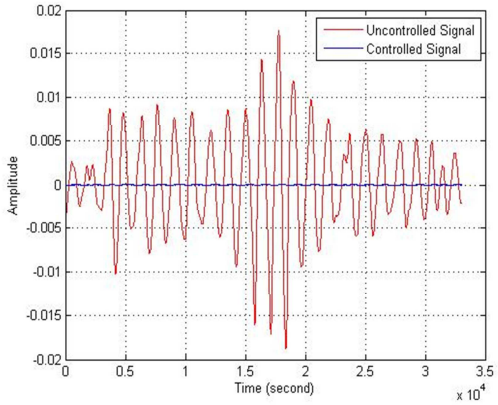

Figure 14 NARX Model Performances With and Without PID Controller.

Journal of Theoretical and Applied Information Technology
10th August 2014. Vol. 66 No.1

ISSN: 1992-8645 www.jatit.org E-ISSN: 1817-3195

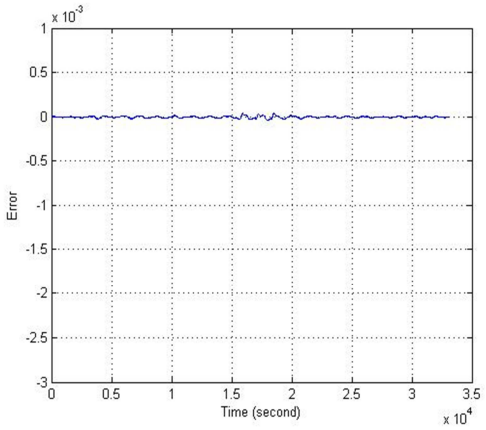

Figure 15 Error Between The Setting Reference Point and Desired Amplitude.

Secondly, according to the Table 6, the outcomes shown that the magnitude for K_P = 3000 at lowest MSE 2.3643×10^{-5}. Also, the outcomes showed that the magnitude for K_I = 750 at lowest MSE 5.7532×10^{-6}. While the magnitude of K_D = -1600 at lowest MSE 3.0368×10^{-6}. Based on Figure 16 and 17, results shown that the PID controller succeeded to suppress the effect VIV comparison with the system performance without controller.

Table 6 PID Parameter Setting By Using MSE

K_P	MSE	K_I	MSE	K_D	MSE
-100	3.0932×10^{-5}	-50	3.1544×10^{97}	-2100	3.2349×10^{-6}
0	3.0347×10^{-5}	0	2.3643×10^{-5}	-2000	3.1585×10^{-6}
100	2.9789×10^{-5}	50	1.6633×10^{-5}	-1900	3.1005×10^{-6}
1000	2.5908×10^{-6}	500	5.8141×10^{-6}	-1800	3.0608×10^{-6}
2000	2.3748×10^{-6}	750	5.7532×10^{-6}	-1600	3.0368×10^{-6}
3000	2.3643×10^{-5}	1000	5.8265×10^{-6}	-1500	3.0526×10^{-6}

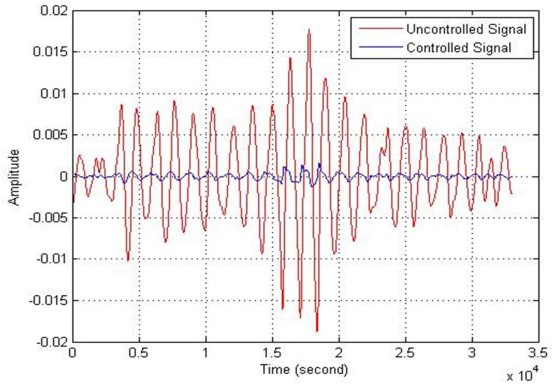

Figure 16 System Performances With and Without PID Controller.

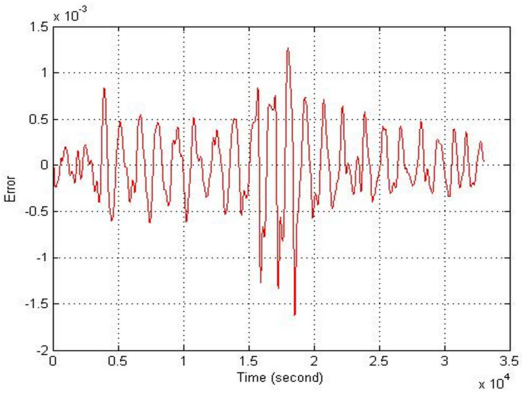

Figure 17 Error between the setting reference point and desired amplitude.

According to all results above, the PID controller has ability to decrease the effect of VIV. But, the performance of PID controller for NARX model was better the ANFIS model where it's recorded the MSE equal $3.669\text{x}10^{-10}$ while the MSE for PID controller for ANFIS model equal 3.0368×10^{-6}. Also, Figure 18 has shown the performance of PID controller on NARX model against ANFIS model.

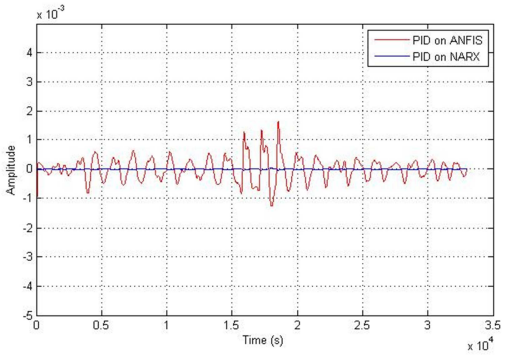

Figure 18 PID Controller Performances On NARX And ANFIS Models.

ISSN: 1992-8645 www.jatit.org E-ISSN: 1817-3195

6. CONCLUSION

The performance of PID controller for NARX and ANFIS system identification models for oscillating cylinder pipe caused by vortex induced vibration has been submitted in this work. The input-output data extracted from the experimental setup for priority research. NARX and ANFIS models are employed to represent the dynamic response of the system after comparing the results by using MSE technique. In system identification, ANFIS model was better than the NARX model to predict the system behavior. Whereas, ANFIS model recorded minimal MSE 2.5635×10^{-13} while NARX model has been recorded MSE 1.2714×10^{-9}. The PID controller proved to be effective to decrease the effect of vortex induced vibration of a pipe cylinder under disturbance load for all models. But the PID performance on NARX model was better than the ANFIS model which recorded the lowest MSE $3.669\text{x}10^{-10}$ while the MSE for PID controller for ANFIS model equal 3.0368×10^{-6}.

7. ACKNOWLEDGMENT

The authors would like to express their gratitude to Minister of Education Malaysia (MOE) and Universiti Teknologi Malaysia (UTM) for funding and providing facilities to conduct this research. This research is supported using FRGS Vote No. 4F395 and UTM Research University grant, Vote No. 05H71

REFERENCES:

[1] C. H. K. Williamson and R. Govardhan, "Vortex-Induced Vibrations," Annu. Rev. Fluid Mech., vol. 36, no. 1, 2004, pp. 413–455.

[2] T. L. Morse and C. H. K. Williamson, "Prediction of Vortex-Induced Vibration Response by Employing Controlled Motion," J. Fluid Mech., vol. 634, 2009, pp. 5-39.

[3] B. V. E. How, S. S. Ge, and Y. S. Choo, "Active Control of Flexible Marine Risers," J. Sound Vib., vol. 320, no. 4–5, 2009, pp. 758–776.

[4] G. S. Baarholm, C. Martin Larsen, and H. Lie,"Reduction of VIV using suppression devices—An empirical approach", Mar. Struct., Vol. 18, No. 7–8, 2005, pp. 489–510

[5] F. Ge, X. Long, L. Wang, and Y. Hong, "Flow-induced vibrations of long circular cylinders modeled by coupled nonlinear oscillators", Sci. China Ser. G Physics, Mech. Astron., Vol. 52, No. 7, 2009, pp. 1086–1093.

[6] R. D. Gabbai and H. Benaroya, "An overview of modeling and experiments of vortex-induced vibration of circular cylinders", J. Sound Vib., Vol. 282, No. 3–5, 2005, pp. 575–616..

[7] L. Cheng, Y. Zhou, and M. M. Zhang, "Controlled Vortex-Induced Vibration on A Fix-Supported Flexible Cylinder in Cross-Flow," J. Sound Vib., vol. 292, no. 1–2, 2006, pp. 279–299.

[8] J. Ro, "Active Control of Flow-Induced Using Feedback Vibrations Velocity Of A Flexible Cylinder Direct," J. Sound Vib., vol. 146, no. 1, 1991, pp. 33–45.

[9] N. M. R. Shaharuddin and I. Z. Mat Darus, "Active Vibration Control of Marine Riser," 2012 *IEEE Conf. Control. Syst. Ind. Informatics*, Sep. 2012, .pp. 114–119.

[10] C.-M. Chang and B. F. Spencer, "Hybrid System Identification For High-Performance Structural Control," Eng. Struct., vol. 56, 2013, pp. 443–456.

[11] N. M. R. Shaharuddin and I. Z. M. Darus, "Fuzzy-PID Control of Transverse Vibrating Pipe Due to Vortex Induced Vibration," *UKSim 15th Int. Conf. Comput. Model. Simul.*, Apr. 2013, pp. 21–26.

[12] N. M. R. Shaharuddin and I. Z. Mat Darus, "System Identification of Flexibly Mounted Cylindrical Pipe Due to Vortex Induced Vibration," *IEEE Symp. Comput. Informatics*, Apr. 2013, pp. 30–34.

[13] H. Peng, T. Ozaki, Y. Toyoda, H. Shioya, K. Nakano, V. Haggan-Ozaki, and M. Mori, "RBF-ARX Model-Based Nonlinear System Modeling And Predictive Control With Application to a Nox Decomposition Process," Control Eng. Pract., vol. 12, no. 2, 2004, pp. 191–203.

[14] J.-S.R. Jang, ANFIS: Adaptiv×10-network-based fuzzy inference system, IEEE Transactions on Systems., Vol. 23, No. 3, 1993, pp. 665-685.

[15] A. R. Tavakolpour, I. Z. Mat Darus, O. Tokhi, and M. Mailah, "Genetic Algorithm-Based Identification of Transfer Function Parameters for a Rectangular Flexible Plate System," Eng. Appl. Artif. Intell., vol. 23, no. 8, 2010, pp. 1388–1397.

[16] M. A. Fadil, I. Z. M. Darus, M. S. Ammoo, and J. Bahru, "Iterative Learning Auto-tuned PID Controller for Micro-Unmanned Air Vehicle," *Conf. on Instrumentation, Measurement, Circuits and Systems*, Apr. 2013, pp. 153–160.